Modeling a Spiking Optical Neuron using Normalized Yamada Rate Equations

Modeling a Spiking Optical Neuron using Normalized Yamada Rate Equations

L. Puts,[1] W. Yao,[1] D. Lenstra[1]

[1] Photonic Integration Group, department of Electrical Engineering, Eindhoven University of Technology, P.O. Box 513, Eindhoven 5600MB, The Netherlands

The sharp increase in artificial intelligence research and the limitations in conventional hardware led to the active research field of neuromorphic computing. An all-optical spiking neural network in photonics is a promising type of neural network closely related to information processing the human brain. A spiking optical neuron and weighting element are at the heart of such a network and can operate at the nanoseconds timescale, orders of magnitude faster than current electronic neural networks. We propose to achieve the integrated all-optical neuron by implementing a saturable absorber next to the gain section in an optical cavity, creating an excitable laser. To better understand the rich dynamics of this device, a simulation study based on the optically-perturbed normalized Yamada rate equations is conducted. The single neuron model shows a non-linear response, stimulus dependent response delay, and temporal integration. This model was then combined with a model for synaptic weighting based on photonic ring resonators to simulate small scale neural network capabilities.

Introduction

Developments in AI research and neural networks and the predictions of the end of Moore's Law have led to developments in the field of neuromorphic computing. The architecture of spiking neural networks (SNN) is inspired by the human brain, which consists of billions of neurons and synapses and processes information using spikes. A two section semiconductor laser shows very similar dynamics compared to these biological neurons, although at a much smaller timescale, and is therefore a suitable candidate to use in a photonic SNN. Recently, different strategies were proposed to achieve a photonic spiking neuron in a fiber laser [1] and in VCSELs [2]. Despite the possibilities to create complex photonic integrated circuits, no complete integration of an all-optical photonic spiking neuron has been realized. In this paper, we focus on the modeling and dynamics of an all-optical neuron by combining the normalized Yamada rate equations with a model for a photonic ring resonator for synaptic weighting to demonstrate an SNN.

Yamada Rate Equations with Optical Injection

An optical neuron should have five properties in order to be used for neuromorphic computations [3], i.e. thresholding, pulse regeneration, a reset state, temporal integration and weighted addition. An important aspect of the first two points is *excitability*, which refers to the non-linear response of a system to an external perturbation. In the case of an all-optical neuron this means that depending on the strength of an optical input stimulus, the neuron produces either a pulse with a fixed amplitude, or it remains at rest. This dynamical property can be introduced in an optical cavity by implementing a saturable absorber next to a gain element. Combined with an element for synaptic weighting and summation, as shown in Fig. 1, all five properties can constructed.

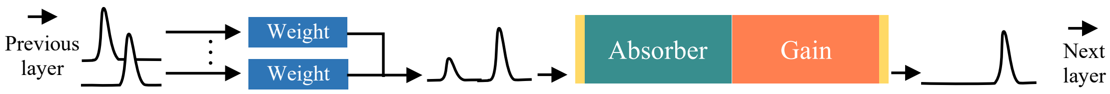

Figure 1: Block diagram of an optical neuron in an SNN, consisting of weighed input pulses injected into the laser

Assuming the optical intensity is constant across the cavity shown in Fig. 1, a lumped-cavity model applies and the dynamics of the two section laser can be described by the Yamada rate equations. This model consists of three coupled differential equations for the gain G, loss Q and intensity I and in non-dimensional form is it as follows [4]:

$$\dot{G} = \gamma_G\,[A - G(t) - G(t)I(t)] \tag{1}$$

$$\dot{Q} = \gamma_Q[B - Q(t) - aQ(t)I(t)] \tag{2}$$

$$\dot{I} = \gamma_I[G(t) - Q(t) - 1]I(t) + \epsilon f(G) + \theta(t) \tag{3}$$

where γ_G and γ_Q are the gain and absorber relaxation rates, respectively, γ_I is the inverse photon lifetime, A the gain bias level, B the absorption bias level, a the saturation parameter, and $\varepsilon f(G)$ the spontaneous emission. In most studies, a stimulus is added as an electrical stimulus to the gain or absorber equation. In our case, an external optical stimulus is applied to the intensity equation via $\theta(t)$.

An example of the numerical solution of Eqs. (1) – (3) over a period of 200 τ_p under a short optical stimulus is shown in Fig. 2 (a) and (b). Initially the intensity is very small, and Eq. (1) and (2) are dynamically decoupled. The applied stimulus is above the excitability threshold, and as a results the intensity inside the cavity increases and the differential equations become coupled. The stimulus saturates the absorber, the optical intensity in the cavity increases exponentially until it reaches its maximum and at the same time the gain depletes, followed by the reset state where the loss and gain recover to their steady state values.

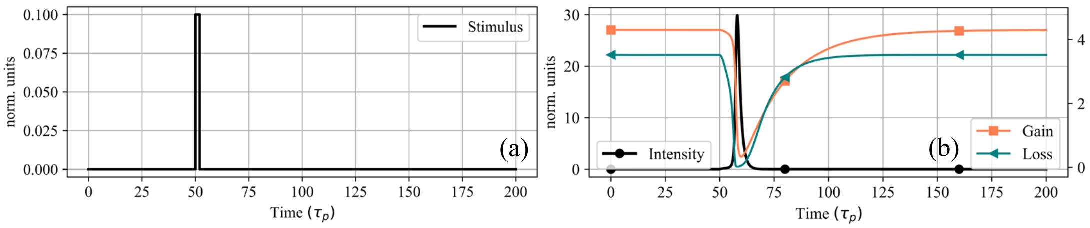

Figure 2: (a) short optical stimulus $\theta(t)$ of intensity 0.06 at t=50 τ_p, (b) response of intensity, gain, and loss to the stimulus. For these simulations, γ_G=0.05, γ_Q=0.1, γ_I=1, A=4.3, B=3.52, a=5.

Simulation Results

To investigate the behavior of the model under different conditions, the influence of the gain and loss control parameters A and B on the laser excitability threshold was considered. The results of this analysis are shown in Fig. 3 (a) and (b), where the amplitude of a pulse in the intensity after a stimulus was recorded for different values of A and B. For all values of A and B, the stimulus was swept from 0 (no injection) to 0.10. From in Fig. 3 (a) it is observed that at A=4.5 and zero stimulus the laser produces a pulse, which means the systems is self-pulsating (region i). When A=4.4 and a small stimulus is applied, no spike was recorded (region ii). For a slight increase in the stimulus amplitude, a step function type threshold in the optical intensity is observed (region iii). This threshold shifts to the right if A is further decreased. Similar behavior is shown in Fig. 3 (b) for values of B. To sum up, these simulations show the thresholding and pulse regeneration properties mentioned in the previous section and thus make it an interesting candidate for an all-optical optical neuron.

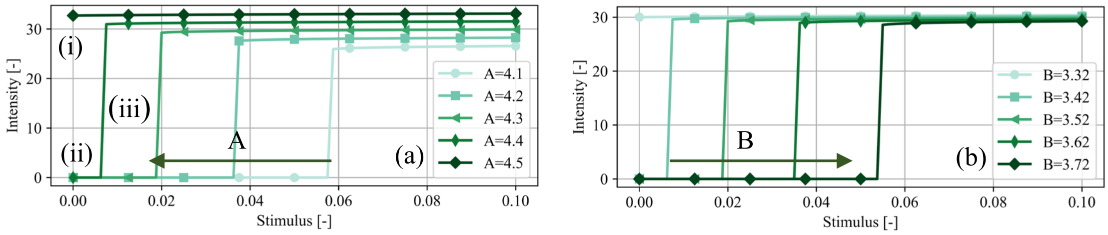

Figure 3: Pulse intensity versus stimulus intensity for various values of the control parameters A and B. In (a), B was fixed to its nominal value of 3.52, in (b), A was fixed to its nominal value of 4.3.

The previous simulations do not provide information on the temporal properties. In the following two simulations, the timing between the stimulus and the response were investigated. Fig. 4 (a) shows the time delay Δt between the stimulus and response as function of the stimulus intensity. The threshold lies around a stimulus intensity of 0.02, which is in accordance with Fig. 2 for A=4.3 and B=3.52. At this stimulus intensity, the time delay is relatively high. This is due to is the difference in time constants between the gain (slow) and absorber and intensity (both fast). For a pulse just at the threshold, the gain is able to increase the intensity just enough to saturate the absorber and generate a pulse. If the stimulus is higher, the intensity is higher, which in turn results in a faster onset of the fast absorber and intensity dynamics, and the time delay decreases.

Next, the time delay between a two consecutive stimuli and the amplitude of the responses is considered. The results of these simulations are depicted in Fig. 4 (b), where the solid line shows the output spike amplitude as a function of the time delay between the first and second stimulus, and the dotted line shows the response of a second stimulus. The solid line is constant over almost the entire simulation, which means there is hardly a difference in timing between the first stimulus and the response. However, both the amplitude as well as the time at which the second spike appears is significantly different compared to the first spike. The second spike appears only after approximately Δt=59 τ_p, at a much lower amplitude. As the time difference increases further, the amplitude approaches the steady state value of the first spike. The reason for this behavior, the *relative refractory period*, is because the gain and loss need a certain amount of time to recover. In this period it is possible to generate a spike, although with a smaller amplitude.

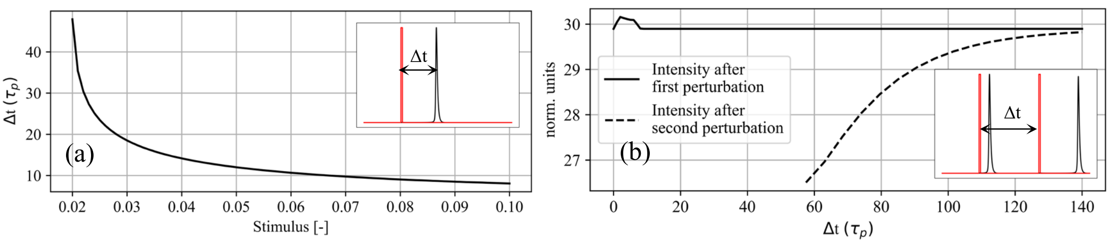

Figure 4: (a) shows the delay between the stimulus and the response. (b) shows the delay between the stimuli and the intensity of the responses. The insets shows the response (black) of a stimuli (red) and Δt.

Small Network Simulation Results

To demonstrate the Yamada model in an SNN, it is combined with a model of a photonic ring resonator. Often used as a spectral filter, this resonator effectively lowers the transmission of a signal [5]. It can thus be used as a synaptic weighting element to control the strength of the connections between neurons. The model for synaptic weighting in the simulation is as follows [5]:

$$T(\phi) = \frac{a^2 - 2ar\cos\phi + r^2}{1 - 2ar\cos\phi + (ar)^2} \tag{4}$$

With detuning ϕ, and r and a the self-coupling and amplitude transmission, respectively. The network simulation is very similar to the situation in Fig. (1), where eight individual pulses are generated using the Yamada model at different times between 0 and 600 τ_p, before each pulse is individually weighted using Eq. (4). The weights are chosen such that the signals contains (i) a spike above threshold, (ii) a sub-threshold train, (iii) a spike below threshold, (iv) a spike slightly above threshold, and (v) two spikes above threshold, closely spaced together in time. The spikes are then summed together to form the input signal of the output neuron in a next layer, which results in the output signal shown in Fig. 5 (b). From these simulations, it is observed that (i) leads to a spike, and due to temporal integration (ii) also leads to a spike at the output, (iii) does not, (iv) does lead to a spike, but because of the lower amplitude the timing between the stimulus and the spike is slightly larger compared to (i), and finally (v) demonstrates the relative refractory period, due to the short time between the two stimuli.

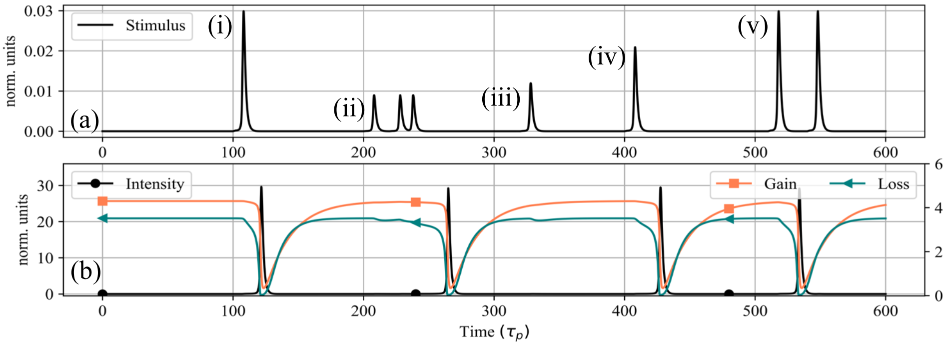

Figure 5: (a) Demonstration of eight different weighted signals after summation, used as the input of a neuron and (b) the corresponding output.

Conclusion

In this work, the dynamics and properties of an optical neuron based on a two section laser were investigated using the normalized Yamada rate equations and a model for a photonic ring resonator. The model shows thresholding, pulse generation, a reset state, temporal integration and weighted addition, all of which are core properties of an optical neuron for neuromorphic computations in a spiking neural network.

Acknowledgement

The authors would like to thank Giuseppe Fortuna for the implementation of the ring resonator in Python.

References

[1] R. Otupiri, B. Garbin, N. G. R. Broderick, and B. Krauskopf, “Excitability in an all-fiber laser with a saturable absorber section,” *J. Opt. Soc. Am. B*, vol. 38, no. 5, p. 1695, May 2021, doi: 10.1364/JOSAB.420204.

[2] J. Robertson, E. Wade, Y. Kopp, J. Bueno, and A. Hurtado, “Toward Neuromorphic Photonic Networks of Ultrafast Spiking Laser Neurons,” *IEEE J. Sel. Top. Quantum Electron.*, vol. 26, no. 1, pp. 1–15, Jan. 2020, doi: 10.1109/JSTQE.2019.2931215.

[3] P. R. Prucnal, B. J. Shastri, T. Ferreira de Lima, M. A. Nahmias, and A. N. Tait, “Recent progress in semiconductor excitable lasers for photonic spike processing,” *Adv. Opt. Photonics*, vol. 8, no. 2, p. 228, Jun. 2016, doi: 10.1364/AOP.8.000228.

[4] M. A. Nahmias, B. J. Shastri, A. N. Tait, and P. R. Prucnal, “A Leaky Integrate-and-Fire Laser Neuron for Ultrafast Cognitive Computing,” *IEEE J. Sel. Top. Quantum Electron.*, vol. 19, no. 5, pp. 1–12, Sep. 2013, doi: 10.1109/JSTQE.2013.2257700.

[5] W. Bogaerts *et al.*, “Silicon microring resonators,” *Laser Photonics Rev.*, vol. 6, no. 1, pp. 47–73, Jan. 2012, doi: 10.1002/lpor.201100017.